

Giant optical activity from the radiative electromagnetic interactions in plasmonic nanoantennast

Cite this: *Nanoscale*, 2013, 5, 3889

Peng Wang,^a Li Chen,^{be} Rongyao Wang,^{*a} Yinglu Ji,^c Dawei Zhai,^a Xiaochun Wu,^c Yu Liu,^a Keqiu Chen^e and Hongxing Xu^{*bd}

We fabricate the linear chains of twisted gold nanorods by a facile chiral molecular templating method. In such a chiral plasmonic system, particle–particle separation distances are in the order of the light wavelength and are much larger than the sizes of individual particles. As a result, the inter-particle interactions in this chiral system are mediated mainly by a relatively weak far-field plasmonic coupling, rather than a strong near-field coupling. However, such a chiral system of twisted gold nanorods show a huge surface plasmon based circular dichroism response, with the highest anisotropy factor around 0.027. This is in contrast to the previous studies in which near-field plasmonic coupling is an indispensable prerequisite to obtain strong optical activity from a chiral plasmonic nanostructure. Our study demonstrates here an alternative strategy for achieving huge chiroptical response of a chiral plasmonic nanostructure based on far-field, radiative electromagnetic interactions of metallic nanoparticles. Theoretical simulations show a satisfactory agreement with the experimental results. This study may provide more flexible ways to design chiral plasmon nanostructures with strong CD responses for various applications.

Received 9th January 2013

Accepted 28th February 2013

DOI: 10.1039/c3nr00148b

www.rsc.org/nanoscale

1 Introduction

Chirality exists ubiquitously in a variety of living and non-living systems. In recent years, rationally designed chiral plasmonic nano/microstructures based on the building blocks of various metallic nanoparticles (NPs) have been of intense experimental and theoretical interest.^{1–7} Compared to the most of natural chiral molecules, artificial plasmonic nanostructures can exhibit very strong chiroptical effects due to a much larger dipole moment of the plasmonic resonance and accordingly a stronger interaction with external light field.² For instance, for individual metallic NPs in chiral environment, the circular dichroism (CD) effect measured through the anisotropy factor (*g*-factor)⁵ is generally at the order of 10^{-3} .^{1,2b} Such an individual chirality occurs presumably in the core or at the interface/surface of metallic NPs.¹ On the other hand, collective chirality arising from the spatially asymmetric arrangement of achiral

metallic NPs^{2–7} can exhibit a much higher value of *g*-factor in the range of 10^{-2} to 10^{-1} at the surface plasmon resonance (SPR) region. This kind of chirality is attributed mainly to the collective plasmon–plasmon interactions of the metallic NPs in a three dimensional (3D) chiral architecture.^{2,8,9} The novel collective electric and photonic properties of such plasmon-based nano/microstructures are anticipated to have promising applications in electronics,³ photonics,¹⁰ and biosensing,¹¹ *etc.*

Under conditions where strong coupling between incident photons and surface plasmons of metallic NPs exists, the type and strength of the collective plasmon–plasmon interactions of the NPs depend strongly on the inter-particle distance *D*.^{11c} At a large inter-particle distance, typically of the order of the light wavelength, far-field, radiative coupling dominates in the particle–particle interactions, following a D^{-1} distance dependence. As the inter-particle distance decreases to a dimension comparable to the nanoparticle size and even smaller, near-field, dipole–dipole coupling prevails and follows a D^{-3} distance dependence.

To date experimental designs have focused mainly on the chiral plasmonic nanostructures working in the near-field coupling regime. The pioneering works by several groups^{4a,5a,6} have demonstrated success in achieving strong collective optical activity from such chiral plasmonic nanostructures. These include a spatially compact organization of gold nanorods (Au NRs) based on twisted fiber bundles,^{5a} a DNA-based plasmonic nanostructure with gold nanoparticles arranged in a tight helix with the gap of the nearest neighboring particles

^aSchool of Physics, Key Laboratory of Cluster Science of Ministry of Education, Beijing Institute of Technology, Beijing, 100081, P R China. E-mail: wangry@bit.edu.cn

^bInstitute of Physics, Chinese Academy of Sciences, Box 603-146, Beijing, 100190, P R China. E-mail: hongxingxu@iphy.ac.cn

^cCAS Key Laboratory of Standardization and Measurement for Nanotechnology, National Center for Nanoscience and Technology, Beijing, 100190, P R China

^dSchool of Physics and Technology, Wuhan University, Wuhan, P R China, 430072

^eDepartment of Applied Physics, Hunan University, Changsha, P R China, 410082

† Electronic supplementary information (ESI) available: Sample preparation details; optical/electron microscopy; circular dichroism and extinction spectra; theory and simulations. See DOI: 10.1039/c3nr00148b

~ 1.2 nm,^{4a} and more recently a 3D chiral plasmonic oligomers of gold particles.⁶ In those chiral structures, the highest g -factor $\sim 10^{-1}$ was reported.⁶ A strong inter-particle interaction mediated by resonant, near-field plasmonic coupling was accepted as an indispensable prerequisite for achieving strong chiroptical response.

In this work, we report an alternative strategy to achieve strong chiroptical response from a chiral plasmonic nanostructure in which the plasmonic coupling works beyond the near-field limit. For the linear chains of twisted Au NRs formed by using lipid-based supramolecular template,⁷ the particle-particle separation distances were manipulated to present a weak plasmonic coupling effect. Interestingly, these linear chains can show a giant plasmonic CD effect. We further show that such an extraordinary plasmonic CD response depends strongly on the aspect ratio of NRs and the inter-particle distance in the linear chains. Theoretical simulations based on the coupled-dipole approximation (CDA) model support fully the experimental observations, and provide a comprehensive understanding on the chiroptical phenomenon arising from far-field, radiative electromagnetic interaction in a chiral plasmonic nanostructure.

II Materials and methods

Linear chains of Au NRs synthesis

Au NRs capped with CTAB with different aspect ratios (2.1, 2.4 and 2.7) were synthesized by using the seed mediated growth method.¹² The linear chains of Au NRs were formed through a hierarchical, cooperative self-assembly/self-organization process in a multiple-component system comprising of preformed Au NRs, surfactants (cetyltrimethylammonium bromide, CTAB), and phospholipid film (1,2-dimyristoyl-*sn*-glycero-3-phosphatidylcholine, DMPC). Firstly, a solution consisting of phospholipids DMPC (Avanti Polar Lipid, 3.5 mg) and small quantities of fluorescent labeled lipid rhodamine DHPE (Invitrogen, 0.02 mg) in 10 mL chloroform was dried to form a thin film by a typical dehydration procedure.¹³ Secondly, the Au NRs-CTAB aqueous solution (~ 1.2 nM, 1.5 mL) and phosphate buffer saline (PBS; 2.5 mL, pH ~ 7.4) were added into the dried lipid film in a flask and hydrated at well above the lipid phase transition temperature (e.g., 65 °C) for 2 h. In this multicomponent system, the molar ratio of CTAB : DMPC was $\sim 0.8 : 1$. After hydration, the sample solution was naturally cooled down to room temperature. Subsequently, the sample solution was centrifuged at 12 000 rpm for 5 min; the precipitates were collected and redispersed in deionized water. The sample solutions with centrifugation treatments were used for spectroscopic and structure characterizations unless otherwise specified. To obtain the linear chains of Au NRs (aspect ratio 2.7) with the relative larger inter-particle distances of ~ 320 nm and ~ 480 nm, 1.5 mL Au NRs-CTAB with the concentrations of ~ 2 nM and ~ 6 nM were used, respectively, in the linear chain preparations. The sample solutions were treated with centrifugation at 8000 rpm for 10 min; the precipitates were collected and redispersed in deionized water. Then the samples were incubated for 12 h to get the supernatant containing twisted Au NRs chains with desirable interparticle distance.

Microstructure characterization

The sample films were prepared by putting a drop of 4 μ L diluted solution on a silicon substrate. After holding still for 2 minutes, excess solutions were removed by filter papers. The samples were then subjected to vacuum-drying (Linkam Scientific Instrument, FDCS 196). Dark-field optical micrographs (Olympus, BX51) of the samples were acquired during the drying process. The dried samples with and without a treatment of gold sputter-coating (30 mA, 20 s) were used to acquire the SEM images of the lipid-based nanotubes and the spatial arrangements of Au NRs, respectively. A scanning electron microscope (SEM, JOEL, JSM-7500F) operating at 2 kV was used to do microstructure analyses.

Optical spectroscopy

Extinction and CD spectra of the linear chains of Au NRs in solution state were acquired using a CD spectrometer (Bio-Logic MOS-450, the spectral range 210–820 nm). The measurements were conducted at room temperature with a 0.5 s scan speed for the solution samples in quartz cell with an optical path of 0.2 cm or 0.1 cm.

III Results and discussion

The lipid-based nanotubes/nanoribbons offer a template for the chiral arrangement of Au NRs to form linear chains. Such supramolecular nano/microstructures based on bilayer-forming amphiphiles have been widely studied as model systems of template-directed arrangements of NPs.¹⁴ Herein, binding of Au NRs into the tubular template may occur through insertion of the freely dispersed CTAB molecules and those adsorbed on the Au NRs into the lipid film,¹⁵ the resulting Au NRs-CTAB-lipid hybrid superstructures in aqueous solution show a good stability.⁷ Compared to the usually used DNA-based templating method, our method based on the lipid tubular template has several advantages: (1) fast and easy-processing, without the complicated and time-consuming procedures of the template preparations, and (2) it is suitable for chiral assembly of relatively large metallic NPs with the sizes at tens of nanometers, which is complementary to the DNA origami method that is limited to small NPs at a few nanometers.^{4a,b} However, similar to the chiral arrangement of metal NPs on the DNA template, a direct observation of chiral geometry of Au NRs arrangements on the lipid-based soft template in solution state is still difficult due to the technical limitations.^{4a,b} For acquiring a high resolution of the spatial arrangement (geometry) of Au NRs in the hybrid superstructure, dried samples were prepared on silicon substrates, and a scanning electron microscope operating at 2 kV was used to do microstructure analyses, in order to prevent the organic-inorganic hybrid structure of the samples from being decomposed by prolonged exposure to high energy electron beams.¹⁶

Microstructure characterization of samples shows a high yield of linear chains of Au NRs on the lipid-based template (see the ESI†). Fig. 1a shows a representative SEM image from the lipid-based chiral arrangement of Au NRs. Linear chains of

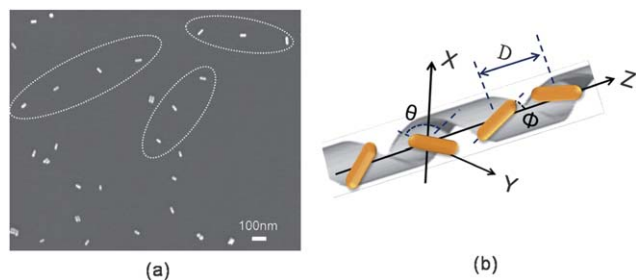


Fig. 1 (a) Representative electron micrograph acquired from a dried and uncoated sample of lipid-based linear chains of Au NRs on silicon wafer by using a SEM operating at 2 kV. The Au NRs (aspect ratio ~ 2.7) are of a mean width of 16.3 ± 2.5 nm and a mean length of 43.6 ± 7.0 nm. Linear chains of Au NRs were denoted by dashed circles. (b) Scheme to illustrate a 3D twisted chain of Au NRs arranged on the lipid-based tubular template in a solution state. D is the center-to-center distance between Au NRs, θ is the azimuth rotation angle between the projections of long axes of neighboring nanorods in the x - y plane, and ϕ is the rotational angle of the long axis of nanorods along the z (helical) axis. With $\phi \neq 0^\circ/180^\circ$, $90^\circ < \theta < 180^\circ$, the chiral geometry of the twisted nanorods chain based on a right-handedness template is optically active.

Au NRs are clearly seen, and some of them show a twisting of the nanorods with mutual orientations with respect to each other. Notably, an important feature of these linear chains is a remarkably large inter-particle distance compared to the sizes of the individual nanorods. From a statistical analysis based on more than 100 linear chains in the SEM micrographs, the average inter-particle center-to-center distance, D , was determined as 250 ± 20 nm. Although the above electron micrographs obtained from the dried samples on the surface of solid substrates display only a two-dimensional (2D) projection of the twisted nanorods, it is reasonable that the twisted Au NRs arranged on the soft lipid-based tubular template in solution state would possess a 3D chiral geometry, as is illustrated in Fig. 1b. In a diluted solution state, the suspended, movable individual linear chains with the twisted nanorods arranged/fixed in a same tubular template would be the major constituent. Such 3D helices of twisted nanorods could present a collective plasmonic CD effect, according to the theoretical predictions.⁸

Spectroscopic measurements were performed for the lipid-based linear chains of Au NRs in solution state. The extinction spectra, particularly the SPR spectroscopy of the Au NRs, provide important information about the dielectric environment and aggregation status of the Au NRs in the linear chains. As is shown in Fig. 2a, CTAB coated Au NRs (aspect ratio ~ 2.7) in a well-isolated state exhibit a transverse plasmon band at 520 nm and a longitudinal plasmon band at 668 nm (red solid line). In comparison, formation of lipid-based linear chains of Au NRs did not show any significant change in the line shape and peak positions of the SPR spectrum (blue solid line). It implies that the dielectric environment and the non-aggregation status of the Au NRs were preserved during the formation of the linear chains. According to previous studies on plasmonic interactions in a linear assembly of such Au NRs,¹⁷ near-field plasmonic coupling would occur when the gaps between neighboring nanorods reach a distance smaller than 30 nm. In

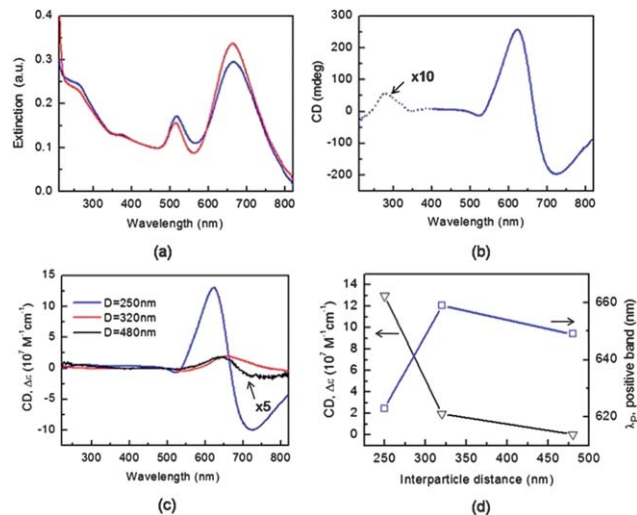


Fig. 2 (a) Extinction spectra acquired from the original CTAB coating Au NRs colloidal solution (red solid line) and from the lipid-based linear chains of Au NRs in a solution state (blue solid line). The concentrations of Au NRs in the two samples are ~ 0.5 nM and ~ 0.3 nM, respectively. (b) CD spectrum collected from the above lipid-based linear chains of Au NRs, including a plasmonic CD signal (solid blue line) in the spectral range of 500–820 nm and an electronic CD signal (dashed blue line) in the spectral region of 210–400 nm arising from the lipid-based supra-molecular template. The electronic CD signal is magnified by 10 for clarity. (c) CD spectra acquired from three kinds of twisted chains of Au NRs with different inter-particle distances (the average values) at 250 ± 20 nm (blue solid line, redrawing of (b)), 320 ± 46 nm (red solid line), and 480 ± 52 nm (black solid line, multiplied by 5 for clarity). Au NRs with the aspect ratio of ~ 2.7 were used in all linear chains. The corresponding concentrations of Au NRs in the three chains are 0.3 nM, 0.4 nM, and 0.8 nM, respectively. (d) Decay of the maximum CD strength and shift of the spectral position with the increase of the inter-particle distance. They are extracted from the positive CD bands in (c), and the peak positions are denoted by λ_p .

our samples, the linear chains of Au NRs have a large inter-particle distance (~ 250 nm), which is in accordance with the above SPR spectral features. It is evident that far-field plasmonic coupling would make a major contribution to the inter-particle interactions of Au NRs in the linear chains.

Such a chiral plasmonic system operating in the far-field plasmonic coupling regime presented a giant CD response at the SPR frequency. As is shown in Fig. 2b, two remarkable chiroptical signatures can be seen: one is located in the near UV region of 210–400 nm, related to the molecular chirality of the lipid-based chiral template (see the ESI[†]); the other is located in the Vis/NIR region, coinciding with the plasmon frequency of Au NRs in the spectral range 500–820 nm. In addition to a weak negative signal at the transverse SPR absorption, the plasmonic CD shows an intense bisignated Cotton effect at the longitudinal surface plasmon modes, with a negative CD band on one side of the longitudinal SPR (at longer wavelengths) and a positive one on the other side (at shorter wavelengths). Strikingly, the g -factor with a maximum value of 0.027 was obtained at the peak position of the positive CD band (~ 630 nm). Such a value is comparable to the highest g -factor values that were reported recently in other relevant chiral plasmonic nanostructures, which operated in the strong near-field plasmonic coupling regime. For instance, a maximum g -factor ~ 0.022

from a helical arrangement of similar Au NRs with neighboring nanorods in close proximity,^{5a} and a maximum g -factor ~ 0.025 from a tight helix of Au–Ag core–shell nanoparticles^{4a} were reported. Note that in the previous study^{5a} helical arrangement of Au NRs (aspect ratio ~ 2.6) with a large inter-particle distance (more than one hundred nanometers) on the twisted bundles was obtained by using a low concentration of Au NRs (~ 0.3 nM) in the chiral hybrid system; but a moderate CD effect with g -factor at ~ 0.002 was obtained.^{5a} In comparison, the g -factor acquired here from the linear chains of twisted Au NRs (with similar aspect ratio and concentration) with a large inter-particle distance arranged on the lipid-based chiral template is one order of magnitude higher than the previous report.

For the Au NRs in a linear chain, the plasmonic coupling between two nanorods depends crucially on their separation distance and relative orientation.¹⁷ In a real system of chiral arrangements of nanorods on a supramolecular template, a distribution of the rotational angles Φ and θ of the twist nanorods (Fig. 1b) exists inevitably.^{5a} Suppose that the distribution of the rotational angles of NRs has a negligible influence on the homogeneity of helix handedness of the linear chains, we focused merely on the determinant role of the inter-particle distance on the plasmonic coupling and consequently on the resulting CD effect from the twisted Au NRs.

The three kinds of linear chains composed of identical Au NRs (aspect ratio ~ 2.7) but with different inter-particle distances were prepared. In these three twisted chains, the average inter-particle distances are 250 ± 20 nm, 320 ± 46 nm, and 480 ± 52 nm, respectively (the SEM images referred to are in the ESI†). Fig. 2c shows the comparison of the plasmonic CD signals (in molar ellipticity) of the three kinds of linear chains. One can see a dramatic change of the CD response both at the signal strength and the spectral position, with the increase of the inter-particle distance. Such changes are depicted more clearly in Fig. 2d for the positive CD bands at short wavelengths. As the inter-particle distance, D , increased from ~ 250 nm to ~ 320 nm, the CD strength decayed sharply by more than a factor of 6, and the spectral position also displayed a pronounced red-shift. With a further increase of D to ~ 480 nm, an approximately 3-fold decay of the CD strength and a blue-shift of the spectral position were observed.

To understand the strong optical activity effect from the linear chains of twisted Au NRs and its dependence on the inter-particle distance in the above experimental results, simulations based on a classic CDA model was conducted (the related details are referred to in the ESI†). This model has been proved to be successful in the prediction of the chiroptical responses from the helical geometry of Au NPs complex.^{4a,5a} Herein we followed a simple chiral model of two Au NRs represented by prolate ellipsoids (inset of Fig. 3a) proposed by Augu e and co-workers,^{8b} by which our chiral plasmonic system was idealized to be a dimer of two dipoles that are oriented along the long axis of each ellipsoid. Although the linear chains of Au NRs in experimental systems would be more complex with, *e.g.*, a distribution of chiral geometry and composition of the nanorods in a chain, such a simple two-particle model can still provide a good description of the

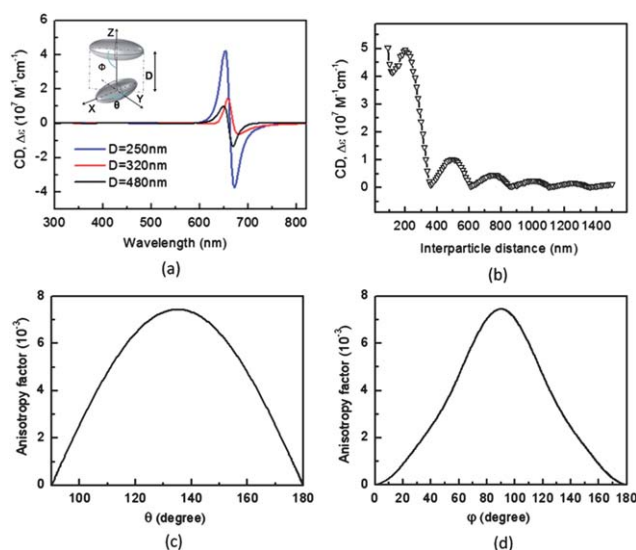


Fig. 3 (a) Simulated CD spectra based on the CDA model for chiral dimer of gold nanorods with an aspect ratio of 2.7 and three different inter-particle distances. The variable inter-particle distances are the same as in Fig. 2c. Inset: the two-particle model of prolate ellipsoids. The long and short semi-axes of the ellipsoids are 21.8 nm and 8.15 nm, respectively. The rotational angles are set as $\theta = 135^\circ$, $\Phi_{NR1} = \Phi_{NR2} = 90^\circ$. (b) Plot of the calculated CD strength at the peak position of the positive band as a function of the inter-particle distance. (c) Plot of the maximum anisotropy factor (at the peak position of positive CD band) as a function of the rotational angle θ in the range from 90° to 180° (with fixed $\Phi_{NR1} = \Phi_{NR2} = 90^\circ$). (d) Plot of the maximum anisotropy factor as a function of the rotational angle ϕ in the range from 0° to 180° (with fixed $\theta = 135^\circ$).

chiroptical phenomenon that is consistent with the experimental observations.

Fig. 3a shows the simulated CD spectra for the three kinds of linear chains of Au NRs whose experimental results are shown in Fig. 2c. Apart from the band-width of the CD spectra, the theoretical simulations show a satisfactory agreement with the experimental results. This includes a similar bisignate line shape for longitudinal surface plasmon modes, a comparable magnitude of the CD strength, as well as the decay of the CD signal and the red-and-blue shift of spectral positions when the inter-particle distance experienced an increase from 250 nm to 320 nm, and then further to 480 nm. Note that the broadening of the SPR spectral band-width is due to the size distribution of nanorods in the experimental results. This would be the major reason for the spectral width observed in the experimental CD spectra, being much broader than those in the theoretical simulations.

Our theoretical simulations also provide a deeper understanding on the inter-particle distance dependence of the plasmonic CD effect. Fig. 3b shows the maximum CD strength (extracted from the calculated positive CD band) as a function of the inter-particle distance D in the range of 100–1500 nm, for the chiral dimer of Au NRs with an aspect ratio of 2.7. With the increase of D , the CD strength displays a damped oscillation with a period of 250 nm, which is one-half longitudinal SP peak wavelength of the Au NRs in aqueous solution with $n = 1.33$. The phase match involved in the resonant plasmon–plasmon interactions of the Au NRs is responsible for this damped

oscillation of the CD strength with the increase of D . In a similar way, the phase match causes a periodical red-shift of the spectral positions with the increase of the inter-particle distance, which shows a sawtooth wave like behaviour (see the ESI†). That is why we experimentally observed a red shift of the spectral position when D increased from 250 nm to 320 nm (in a same period), while a blue-shift of the spectral position when D increased further to 480 nm (in another period).

Note that the CD effect would not vanish even at a very large D . For instance, a CD strength of $10^6 \text{ M}^{-1} \text{ cm}^{-1}$ would appear at $D = 1500 \text{ nm}$. It implies that, although the plasmonic coupling between relatively large separated NRs is very weak, the CD effect can be pronounced due to a proper phase match involved in the far-field electromagnetic interactions between chiral arranged nanorods. In addition, our calculations reveal that, in the case of far-field coupling, a rapid decay of the CD strength from 10^7 to $10^6 \text{ M}^{-1} \text{ cm}^{-1}$ would occur when D varies from 200 to 330 nm, followed by a slow decay of CD strength. This trend fully supports our experimental observations, as shown in Fig. 2d.

In addition to the inter-particle distance, a proper distribution of the rotational angles, Φ and θ , in the twist chains of nanorods is required for obtaining strong CD strength. Numerical simulations were conducted for investigating the dependence of the maximum anisotropy factor (at the peak position of positive CD band in Fig. 3a) on the rotational angles of nanorods, as is shown in Fig. 3c and d. The highest g -factor value, *i.e.*, the most intense CD response, is obtained for $\theta = 135^\circ$, $\Phi_1 = \Phi_2 = 90^\circ$, then the g -factor values gradually decrease with the rotational angles deviating from the above optimal values. Eventually the CD effect would disappear when θ approaches $90^\circ/180^\circ$ or Φ approaches to $0^\circ/180^\circ$, as such spatial arrangements of the nanorods dimer are of achiral geometry. Furthermore, our results suggest that, although occurrence of CD effect from the twisted chain of nanorods would not strongly depend on the rotational angles, a proper distribution of the chiral geometry, for instance, $105^\circ < \theta < 164^\circ$ and $53^\circ < \Phi < 127^\circ$ (the corresponding spectral FWHM in Fig. 3c and d, respectively) would be favored by a strong optical activity of the twisted chains.

We further examined the role of the aspect ratio of Au NRs in the induction of a strong plasmonic CD strength in the linear chains. The three types of gold nanorods that have a nearly constant particle volume but with different aspect ratios (2.1, 2.4 and 2.7) were used to obtain three kinds of linear chains. Fig. 4a shows the normalized CD spectra from these linear chains. As is expected, the spectral peak positions of these CD signals show red-shift accordingly with the SPR frequency of the nanorods. Moreover, with the increase of the particle aspect ratio, a linear growth of the maximum g -factor value (at the peak of the positive CD band) in the range of 10^{-3} to 10^{-2} was observed (Fig. 4b). These results are consistent with the theoretical calculations (see the ESI†). The pronounced enhancement of the CD strength with an increase of the particle aspect ratio can be understood in terms of an increased light–plasmon interaction in a larger aspect ratio of the particle.^{8b} It suggests that a larger particle aspect ratio would be another important

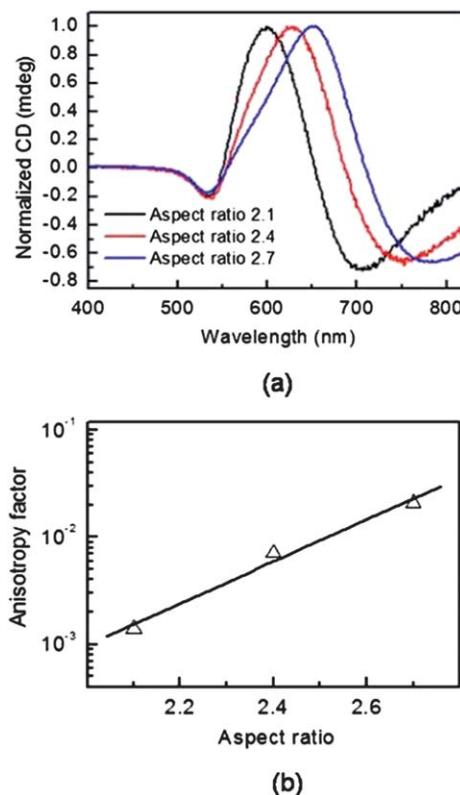


Fig. 4 (a) Normalized CD spectra acquired from three kinds of twisted chains composed of different aspect ratios of Au NRs at ~ 2.1 (black solid line), ~ 2.4 (red solid line), and ~ 2.7 (blue solid line). (b) Maximum g -factor (at the peak positions of the positive CD bands) acquired from the three kinds of twisted chains of Au NRs after centrifugation treatments. A guide-line (dashed line) is used to show an enhancement of g -factor with the increase of the particle aspect ratio.

factor to facilitate a strong optical activity effect from the linear chains of Au NRs.

IV Summary and conclusions

We have demonstrated that a giant optical activity effect can be achieved from the linear chains of twisted Au NRs in which collective plasmon–plasmon interactions work beyond the near-field limit. Our findings highlight here that, apart from a larger aspect ratio of the particles that facilitates strong light–plasmon interactions, a proper chiral geometry with an optimal inter-particle distance that is favored by a well phase matching involved in the far-field electromagnetic interactions would be a key issue for achieving ultrahigh plasmonic CD response from this kind of chiral plasmonic nanostructure. This study may offer a new direction for the exploitation of dipole radiative interaction effects of chiral plasmonic nanoantennas for various bioscience and biomedicine applications.

Acknowledgements

We would like to thank Mr S. P. Zhang and Dr L M Tong from the Institute of Physics, Chinese Academy of Sciences for their valuable discussions and kind help with this work. This work

was supported by the National Natural Science Foundation of China (11174033, 91127013, 10874233, 11004237), MOST Grant (no. 2009CB930700), and “Knowledge Innovation Project” (KJCX2-EW-W04) and Youth Innovation Promotion Association of CAS.

Notes and references

- 1 (a) C. Gautier and T. Bürgi, *ChemPhysChem*, 2009, **10**, 483; (b) C. Noguez and I. L. Garzón, *Chem. Soc. Rev.*, 2009, **38**, 757; (c) Y. S. Xia, Y. L. Zhou and Z. Y. Tang, *Nanoscale*, 2011, **3**, 1374.
- 2 (a) A. O. Govorov, Y. K. Gun'ko, J. M. Slocik, V. A. Gérard, Z. Y. Fan and R. R. Naik, *J. Mater. Chem.*, 2011, **21**, 16806; (b) A. Guerrero-Martínez, J. L. Alonso-Gómez, B. Auguié, M. M. Cid and L. M. Liz-Marzán, *Nano Today*, 2011, **6**, 381.
- 3 (a) M. Yang and N. A. Kotov, *J. Mater. Chem.*, 2011, **21**, 6775; (b) A. Guerrero-Martínez, M. Grzelczak and L. M. Liz-Marzán, *ACS Nano*, 2012, **6**, 3655; (c) S. J. Tan, M. J. Campolongo, D. Luo and W. L. Cheng, *Nat. Nanotechnol.*, 2011, **6**, 268; (d) W. Chen, A. Bian, A. Agarwal, L. Liu, H. Shen, L. Wang, C. Xu and N. A. Kotov, *Nano Lett.*, 2009, **9**, 2153.
- 4 (a) A. Kuzyk, R. Schreiber, Z. Y. Fan, G. Pardatscher, E. Roller, A. Högele, F. C. Simmel, A. O. Govorov and T. Liedl, *Nature*, 2012, **483**, 311; (b) X. B. Shen, C. Song, J. Y. Wang, D. W. Shi, Z. G. Wang, N. Liu and B. Q. Ding, *J. Am. Chem. Soc.*, 2012, **134**, 146; (c) W. J. Yan, L. G. Xu, C. L. Xu, W. Ma, H. Kuang, L. B. Wang and N. A. Kotov, *J. Am. Chem. Soc.*, 2012, **134**, 15114.
- 5 (a) A. Guerrero-Martínez, B. Auguié, J. L. Alonso-Gómez, Z. Dzolic, S. Gómez-Grana, M. Zinic, M. M. Cid and L. M. Liz-Marzán, *Angew. Chem., Int. Ed.*, 2011, **50**, 5499; (b) F. Leroux, M. Gysemans, S. Bals, K. J. Batenburg, J. Snauwaert, T. Verbiest, C. Van Haesendonck and G. Van Tendeloo, *Adv. Mater.*, 2010, **22**, 2193.
- 6 M. Hentschel, M. Schäferling, T. Weiss, N. Liu and H. Giessen, *Nano Lett.*, 2012, **12**, 2542.
- 7 R. Y. Wang, H. L. Wang, X. C. Wu, Y. L. Ji, P. Wang, Y. Qu and T. S. Chung, *Soft Matter*, 2011, **7**, 8370.
- 8 (a) Z. Y. Fan and A. O. Govorov, *Nano Lett.*, 2010, **10**, 2580; (b) B. Auguié, J. L. Alonso-Gómez, A. Guerrero-Martínez and L. M. Liz-Marzán, *J. Phys. Chem. Lett.*, 2011, **2**, 846.
- 9 A. Christofi, N. Stefanou, G. Gantzounis and N. Papanikolaou, *J. Phys. Chem. C*, 2012, **116**, 16674.
- 10 (a) J. B. Pendry, *Science*, 2004, **306**, 1353; (b) H. Wei, Z. X. Wang, X. R. Tian, M. Käll and H. X. Xu, *Nat. Commun.*, 2011, **2**, 387; (c) Y. Hadad and B. Z. Steinberg, *Phys. Rev. Lett.*, 2010, **105**, 233904; (d) A. Christofi, N. Stefanou, G. Gantzounis and N. Papanikolaou, *Phys. Rev. B: Condens. Matter Mater. Phys.*, 2011, **84**, 125109.
- 11 (a) E. Hendry, T. Carpy, J. Johnston, M. Popland, R. V. Mikhaylovskiy, A. J. Laphorn, S. M. Kelly, L. D. Barron, N. Gadegaard and M. Kadodwala, *Nat. Nanotechnol.*, 2010, **5**, 783; (b) N. A. Abdulrahman, Z. Fan, T. Tonooka, S. Kelly, N. Gadegaard, E. Hendry, A. O. Govorov and M. Kadodwala, *Nano Lett.*, 2012, **12**, 977; (c) N. J. Halas, S. Lal, W. S. Chang, S. Link and P. Nordlander, *Chem. Rev.*, 2011, **111**, 3913.
- 12 B. Nikoobakht and M. A. El-Sayed, *Chem. Mater.*, 2003, **15**, 1957.
- 13 D. D. Lasic, in *Liposomes: from physics to applications*, Amsterdam, New York, 1993.
- 14 (a) T. Shimizu, M. Masuda and H. Minamikawa, *Chem. Rev.*, 2005, **105**, 1401; (b) R. R. Price, W. J. Dressick and A. Singh, *J. Am. Chem. Soc.*, 2003, **125**, 11259; (c) S. L. Burkett and S. Mann, *Chem. Commun.*, 1996, 321.
- 15 (a) T. Harada, F. Simeon, J. B. Vander Sande and T. A. Hatton, *Phys. Chem. Chem. Phys.*, 2010, **12**, 11938; (b) C. J. Orendorff, T. M. Alam, D. Y. Sasaki, B. C. Bunker and J. A. Voigt, *ACS Nano*, 2009, **3**, 971.
- 16 J. George and K. G. Thomas, *J. Am. Chem. Soc.*, 2010, **132**, 2502.
- 17 (a) P. K. Jain, S. Eustis and M. A. El-Sayed, *J. Phys. Chem. B*, 2006, **110**, 18243; (b) P. Pramod and K. G. Thomas, *Adv. Mater.*, 2008, **20**, 4300; (c) H. J. Chen, L. Shao, Q. Li and J. F. Wang, *Chem. Soc. Rev.*, 2013, **42**, 2679.